Formation and Breakup of Ligaments from a Rotary Bell Cup Atomizer

M. Shirota*, Y. Hatayama*, T. Haneda*, T. Inamura*, M. Daikoku†, Y. Saito‡, H. Aoki‡
*Course of Intelligent Machines and Engineering, Graduate School of Science and Technology, Hirosaki University, Hirosaki, Aomori, Japan
†Department of Mechanical Engineering, Faculty of Engineering, Hachinohe Institute of Technology, Hachinohe, Aomori, Japan
‡Department of Chemical Engineering, Graduate School of Engineering, Tohoku University, Sendai, Miyagi, Japan

Abstract

Formation and breakup of ligament from a high speed rotary atomizer was investigated by using experimental observation with short flash exposure and theoretical modeling. With the aid of digital image processing, property of ligaments including trajectory, diameter and length were defined quantitatively. The droplet size distribution was measured by using particle size analyzer based on Fraunhofer diffraction theory. Conclusions are summarized as follows: (1) The liquid film is split over the grooves at the edge of a bell cup. (2) The diameter of ligament root is determined by the width of the split film in the case of lower rotational speed of bell cup, while it is determined by the instability of liquid film on the peripheral edge of cup in the case of higher rotational speed. (3) Simple kinetic model on ligament stretching motion provides good estimation on the thinning rate of ligament diameter along its axis. (4) Webers theory for the breakup model of viscous ligament well estimate the diameter of droplet of liquids having viscosity from 30 to 100 mPa·s within the uncertainty of present measurements.

Introduction

Rotary bellcup atomizers are widely used in industrial painting especially in automobile painting. The characteristics of this painting include high efficiency, large processing area per unit time and excellent quality of finishing. In a rotary atomizer, paint liquid supplied on the inner surface of the bell-shaped cup is firstly spread into thin film due to centrifugal force, and then issued as ligaments at the peripheral edge of the cup. The ligaments are further elongated and finally collapsed into droplets.

In previous studies, the effect of geometrical paramter of rotating disks and cups were investigated through detailed photographic observation by Tanasawa et al.[1]. They also found the critical flow rate for several mode of atomization from rotating disk or cup without grooves. in the work of Corbeels et al.[2], the contributions of operating condition and liquid property on the size of droplets produced were further investigated. They found that in the range of high rotational speed the liquid property, such as viscosity, surface tension and density, has small effect on the diameter of droplets produced. Theoretical formulations on ligament formation with and without drag of surrounding air were respectively derived by Kayano and Kamiya [3], and Matsumoto and Takashima [4].

In our previous study [5], we investigated liquid flow patterns on the inner surface of a rotary bell cup atomizer and the effect of these flow patterns on the liquid breakup from a rotary bell cup. We classified the breakup patterns into several patterns such as droplet, ligament, fine ligament and film breakup, and clarified the boundary for these breakup patterns by using bell cup with or without groove at the edge. Our previous analysis led to a conclusion that with the groove the formation of ligament becomes substantially different from that without grooves; with grooves we found out that very fine ligaments forms from a rotary atomizer especially when rotating speed is beyond 10000 rpm regardless of liquid supply rate. However the mechanisms on the formation of such fine ligaments from a high-speed rotary bell cup atomizer with grooves have not well understood.

In the present study, we investigate the theoretical model for the formation of ligament focusing especially on the effect of groove. In experiment, the magnification rate of photography is increased compared to our previous investigation in order to capture, in more detail, the geometrical parameters of both the film at the grooves and the ligaments issued from a bell cup.

Experimental Methods

Setup and material

Figure 1 shows the schematic of the experimental setup. A bell-shaped cup ⑧ is mounted on an axis of an air bearing motor ⑦. The rotational speed of the bell cup is counted by using a laser reflectometer③, and is kept

*Corresponding author: mshirota@cc.hirosaki-u.ac.jp

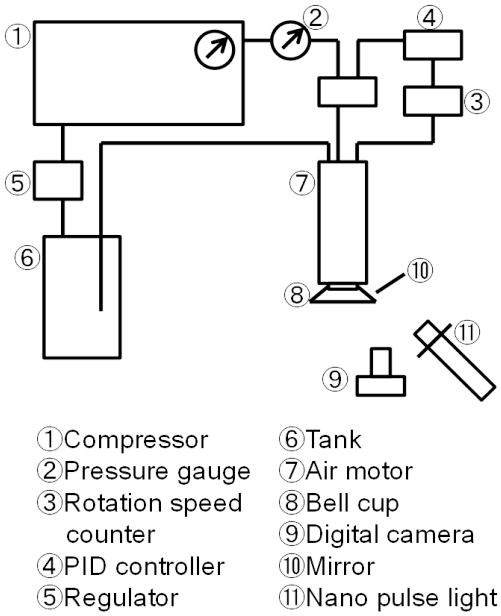

Figure 1. Schematic of experimental setup.

Table 1. Physical properties of test liquids.

Liquid	Viscosity	Density	Surface tension
	10^{-3} Pa · s	kg/m^3	10^{-3} N/m
1	24	1053	26.8
2	70	1132	30.8
3	118	1150	34.2

constant at a certain speed by a PID controller④. Test liquid is pressurized by a compressor ① and supplied through liquid supply ports on the inner surface of the bell cup.

The bell cup used in the present study is about 70 mm in diameter. Liquid supply ports are arranged radiately around the center of the bell cup. The bell cup is also provided with approximately 600 grooves at the peripheral edge.

The rotational speed of bell cup was varied from 5000 to 30000 rpm, while liquid supply flow rate was kept constant at Q=300 ml/min every run. For test liquids, we used glycerin ethanol solution of three different mixing ratio. Main difference in physical properties of these liquids is viscosity, that are 24, 70 and 118 mPa·s as shown in table 1.

Digital imaging and image processing

The shadow of the ligaments were captured using a digital still camera ⑨(D300s, Nikon) with a 180 nsec pulse light⑪(NPL-5, Sugawara Laboratories Inc.) reflceted by a mirror⑩. A macro lens of 105 mm focal length with bellows were attached to the camera in order to magnify the image. The resolution of image was 4288 $\times$ 2848 pixels, magnification rate was 2 μm /pix while the actual optical resolution was found to be approximately 5 μ m after spatial resolution tests with a standard clearance chart.

In image processing, we utilized MATLAB Image Processing Toolbox. Figure 2 shows typical processes of the present image processing. Starting from the original image(a), the peripheral edge of the bell cup is first determined (b). Then the boundary of ligament is determined by an edge detection method, Canny method (c). Finally, local curvature, which corresponds to local diameter, of ligament is calculated by fitting a circle that touches the boundaries (d).

Theoretical Modeling on Ligament Formation

As shown schematically in figure 3, the formation of ligament is divided into mainly the following five processes. In the first process, film thinning due to centrifugal force take place. The film is then split over the grooves at the edge of the bell cup into approximately six hundreds of films, the number of which corresponds to that of grooves. As the split liquid reaches to the peripheral edge, it starts to stretch with its basis attached on the edge. Hereafter we refer this attaching part of ligament as ligament root. The issued ligaments are then stretched resulting in more thinning in diameter toward the tip. The last process involves the breakup of ligaments into droplets. We developed in the following the theoretical models for these process of film split, root formation, stretching and break up of ligament.

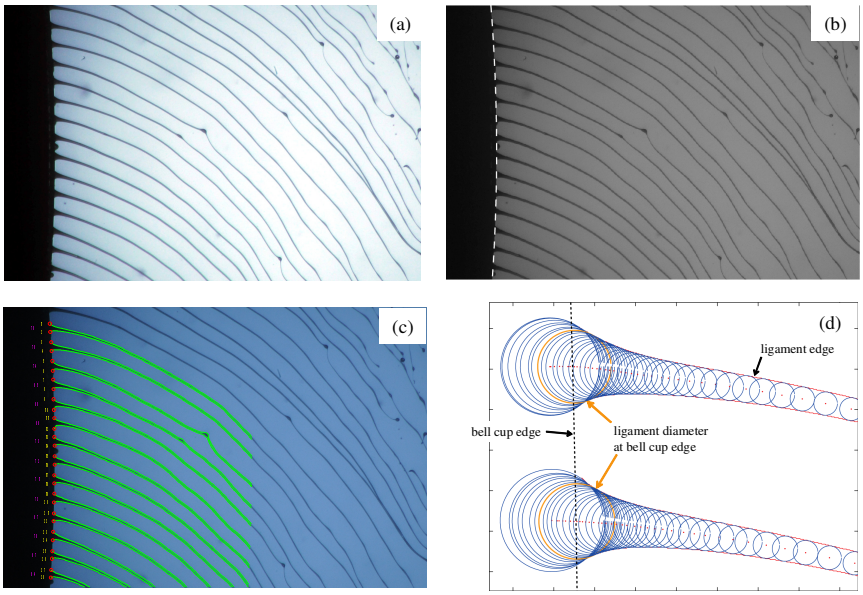

Figure 2. Typical processes in image processing.

Thickness of ligament at the bellcup edge

In the formation of ligament root, liquid film is firstly split over the grooves into small portion of films when the film thickness in the groove δ_g is smaller than the groove depth h_g, see Fig. 4. We model this split of liquid film in order to obtain the width of the film w_f at bell cup edge. The length of liquid film overflown the groove L_o is simply the difference between groove length L_g and the length of film under the groove L_f,

$$L_o = L_g - L_f. \tag{1}$$

By using Pythagorean theorem, L_f can be defined as,

$$L_f = \sqrt{(R_c - \delta_g)^2 - (R_c - h_g)^2}, \tag{2}$$

where $R_c$is the radius of cutter for the fabrication of groove. Note here that δ_g does not correspond to the film thickness on a rotating disk without groove δ_0 [6],

$$\delta_0 = \left(\frac{3\nu Q}{2\pi R^2 \omega^2}\right)^{1/3}, \tag{3}$$

but is a function of both δ_0 and the geometrical parameter of the cross section of groove. The width of the film may be defined by assuming the cross section of groove having triangle shape with a vertical angle of β as,

$$w_f = 2L_o \tan\left(\frac{\beta}{2}\right). \tag{4}$$

If we neglect second order higher terms on δ_g and h_g, then Eq. (2) reduces to

$$L_f \approx \sqrt{2R_c(h_g - \delta_g)}, \tag{5}$$

which gives the approximation on w_f as

$$w_f \approx \sqrt{\frac{2R_c}{h_g}} \tan\left(\frac{\beta}{2}\right) \delta_g. \tag{6}$$

This approximate model shows linear relation between w_f and δ_g.

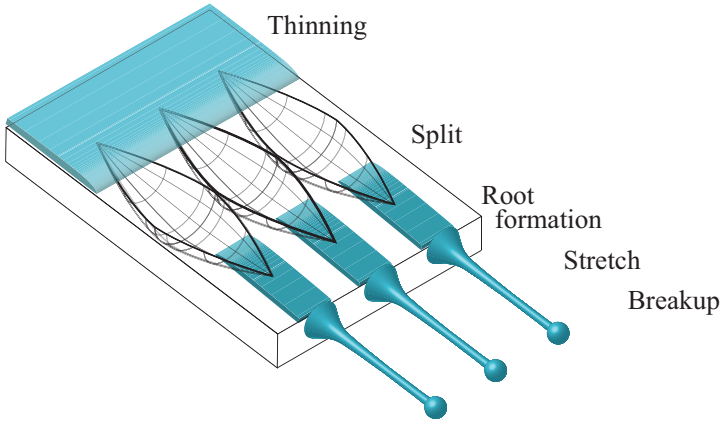

Figure 3. Schematic diagram of ligament formation from a rotary bell cup with groove.

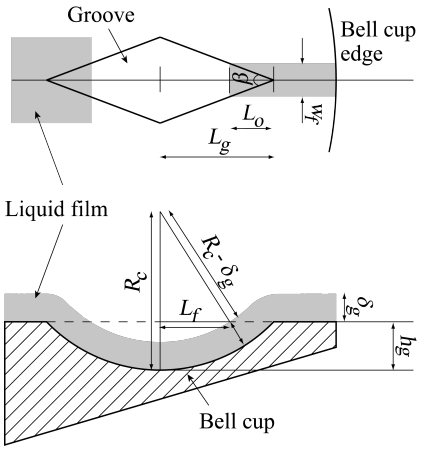

Figure 4. Schematic of liquid films split over grooves.

stretch of ligament

Liquid film on a rotary atomizer has both tangential and radial velocity at the atomizer edge. While the characteristic tangential component v_θ is simply given as rotational speed of bell cup, the radial one can be estimated by theoretical expression on the maximum radial speed at bell cup edge [6],

$$v_{r,max} = \left(\frac{9\omega^2 Q^2}{32\pi^2 \nu R} \right)^{1/3}. \tag{7}$$

Because with our typical experimental condition v_r/v_θ is about 0.0003, we neglect the effect of radial component of liquid film velocity in the following analysis. With only the tangential velocity at the injection, kinematic model without drag of surrounding air [4] gives the following system of equations on the trajectory of ligament:

$$\begin{aligned} x &= R\cos(\omega t) + R\omega t \sin(\omega t) \\ y &= R\sin(\omega t) - R\omega t \cos(\omega t) \end{aligned} \tag{8}$$

Liquid velocity in a ligament is given by

$$V_L = \sqrt{\left(\frac{dx}{dt}\right)^2 + \left(\frac{dy}{dt}\right)^2} = R\omega^2 t. \tag{9}$$

Using the breakup time t_b at which ligament collapses into droplets, we can write the break up length of ligament L_b as follows:

$$L_b = \frac{1}{2} R\omega^2 t_b^2. \tag{10}$$

This equation shows that the ligament accelerates from the root toward the tip with constant acceleration of $R\omega^2$ when observed from a rotary bell cup. If we eliminate stretching time from equations (9) and (10), we can obtain relation between ligament velocity and length L

$$V_L = \sqrt{2R\omega^2 L}. \tag{11}$$

The combination of this equation with equation of continuity gives ligament diameter at length L

$$d_L = d_{L,0}\sqrt{\frac{V_{L,0}}{V_L}} = d_{L,0}\sqrt{\frac{V_{L,0}}{2R\omega^2}} L^{-1/4}. \tag{12}$$

This equation reads that ligament diameter decreases as $d_L \sim L^{-1/4}$.

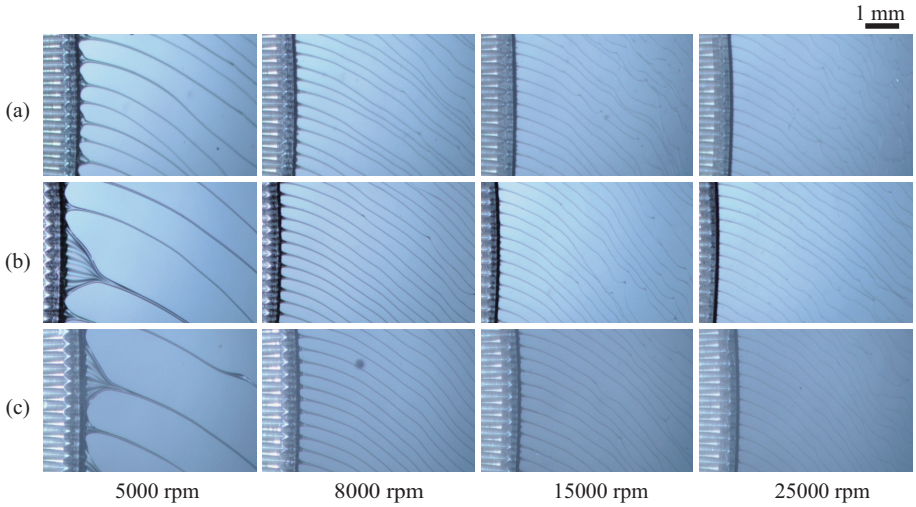

Figure 5. Photographs of ligaments issued from a rotary bell cup. (a)Liquid 1, (b)liquid 2, (c)liquid 3.

breakup of ligament into droplets

From Weber's theory, the droplet diameter disintegrated from the ligament tip of $d_{L,b}$ in diameter can be written as,

$$D = 1.88 d_{L,b}(1 + 3Oh)^{1/6}, \tag{13}$$

where Oh is Ohnesorge number

$$Oh = \frac{\mu}{\sqrt{\rho \sigma d_{L,b}}}. \tag{14}$$

Results and Discussion

Overall characteristics of ligament formation

Figure 5 shows typical photographs of ligaments ejected from the edge of a rotary bell cup. In this figure, it is clearly shown that both difference in liquid viscosity and rotational speed greatly affect the formation of ligament; with the increase in viscosity and decrease in rotational speed, which correspond to observing from top to bottom in Fig. 5 and from right to left respectively, thickness of ligament increases. It is also found that in higher rotational speeds, ligaments are ejected from every groove properly, while in the lower rotational speed of 5000 rpm several ligaments merged after the ejection. This unsystematic coalescence of ligaments varies the thickness of ligaments which changes both the inertia and viscous drag of surrounding air and thus results in the variance of ligament trajectory.

Thickness of ligament at the bellcup edge

As shown in the previous section, the coalescence of ligament just after the bell cup edge strongly affects the following formation of ligaments. We thus in this section focus on the formation of ligament root since its thickness has strong influence on both the coalesce and further stretching of ligaments.

In Fig. 6, magnified images of the ligaments at the bellcup edge are shown. In this photography, we shed a flash light on the front surface of the bell cup in addition to the back light. It is found in figure 6 (a) that when rotational speed is low the liquid film entirely overflows the groove and wets over around the edge of the cup. With higher rotational speed, in contrast, the edge part is partially wet, shown as dark region between arrows in Figs. 6 (b), (c) and (d), by liquid film split over the grooves. By using image processing with these figures, we defined the width of liquid film split over the grooves. We defined the width as the length that lies between the local maximum intensity gradient of image intensity in radial direction from the tip of the groove to the edge of the bell cup. Figure 7 shows the relation between the film width w_f of liquids of different viscosity and bell cup rotational speed N. It is shown in this figure that w_f decrease monotonically with increasing N and decreasing viscosity above N = 8000 rpm. Note here that error bars indicate the interval of standard deviation from the mean value of data set of typically ten data.

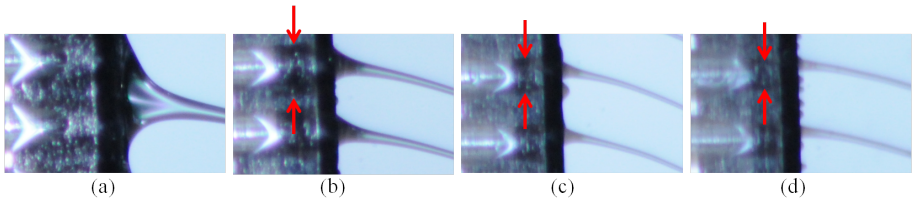

Figure 6. Magnified images of ligament root at bell cup edge, of liquid 1, with different rotational speed of (a) 5000, (b)8000, (c)15000 and (d)25000 rpm.

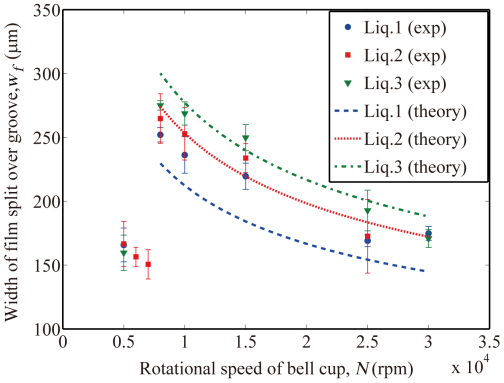

Figure 7. Relation between width of film split over groove and rotational speed of cup.

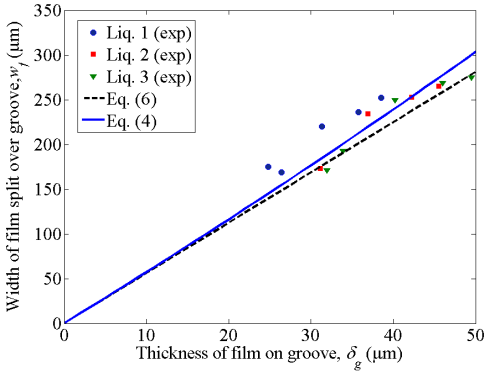

Figure 8. Relation between width and thickness of film split over groove.

The dashed lines in Fig. 7 show film width estimated using eq. (4) where the effect of rotational speed N = $60 \cdot \omega/2\pi$ and liquid viscosity $\nu = \mu/\rho$ are taken into account through the expression for film thickness just before the groove δ_0 written in Eq. (3). The theoretical expression well estimates such characteristics of film width as decrement with increasing rotational speed and with decreasing liquid viscosity. However qualitative agreement is not achieved. Possible reason for this discrepancy arises from the definition of film thickness measured through image processing. It is also noteworthy that in Fig. 7 for $N < 8000$ w_f is smaller than that for $N \geq 8000$. This is because the film is not properly split but overflown the groove and forms a continuous sheet of film even at the edge of bell cup. In that condition, ligaments tend to merge just after the bell cup edge.

The theoretical model for w_f expressed by Eq. (4) is based on the assumption that the liquid film is first spread due to high-rotational speed of bell cup to have thickness of δ_0 just before the groove and then δ_g in the groove. The thickness of liquid film as well as geometric parameter of groove determine the film width overflown the groove. In order to confirm this basic assumption for the calculation of w_f, in Fig. 8 we plot experimentally obtained w_f, which is already shown in Fig. 7, against δ_g which is determined theoretically by using experimental conditions. As shown in this figure, w_f and δ_g is almost in a linear relation, which is well estimated by theoretical model using Eq. (4) and the approximate model given by Eq. (6).

Let us now consider the relation between w_f and the diameter of ligament root d_0. A close observation of Fig. 6 shows that at lower rotational speed, such as N = 8000 rpm, $w_f \simeq d_0$. At higher rotational speed however $w_f > d_0$ and one or two droplets are found between ligaments on the peripheral edge. This observation suggests that there exists two mechanisms that rules the number of ligaments and thus d_0: one is the number of grooves which dominates in relatively low rotational speed, and the other arises from the instability of liquid sheet on the peripheral edge at high rotational speed due to high centrifugal acceleration. The number of ligaments due to the instability N_l is provided in the following semi-empirical equation [6],

$$N_l = 0.574 Re^{1/3} We^{1/4}. \tag{15}$$

We then developed the following model for d_0 where film of w_f is split into several roots for ligament and droplets on the peripheral edge by instability,

$$d_0 = \frac{w_f}{\max(\mathrm{N_l}/\mathrm{N_g}, 1)}, \tag{16}$$

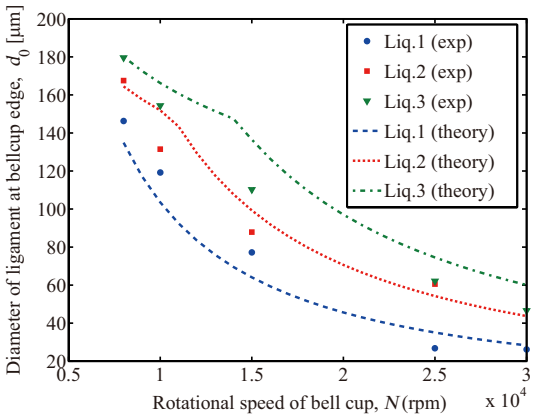

Figure 9. Comparison between theoretical estimaion and experimental results on thickness of ligament root.

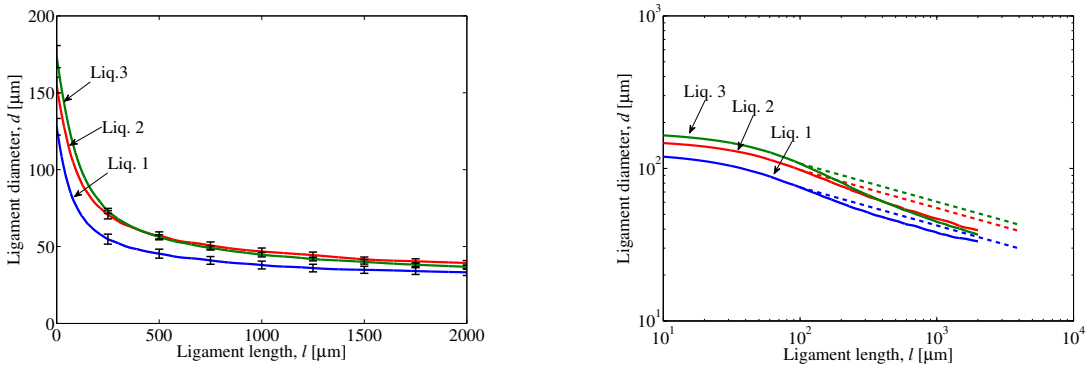

Figure 10. Ligament diameter along its axis.

where N_g is the number of grooves and max(a,b) is a function returning maximum value between a and b. By using the max function, the smallest number of ligaments is limited to N_g.

In Fig. 9, the model estimation on d_0 given by Eq. (16) are compared with experimental results. This figure shows the model estimation is in good agreement with experimental results, which confirms our hypothesis that the formation of ligament root are controlled by either the groove of the atomizer or the instability of liquid sheet by high-speed rotation. It should be stressed however that even though droplets may be formed between ligaments, only a single ligament is stretched per each groove. Therefore the number of stretched ligaments equals N_g even for higher rotational speed.

Stretching motion of ligament

The variation in diameter of ligament along its axis is determined in the image processing shown in previous section, and is compared with model estimation given by Eq. (12). Results are shown in Fig. 10 against ligament length from the root for liquids 1, 2 and 3 of different viscosity. For each viscosity, approximately ten ligaments are sampled. Error bars in the left hand side of Fig. 10 show the standard deviation of the sampled ligaments. Although ligament diameter are determined at points arranged in geometrical progression, as explained in the chapter on image processing, we shows error bars at some points of characteristic length after interpolation. Theses sets of error bars show such small deviation in diameter as less than 10 % of mean diameter all along the axis.

If we look at the variation in mean diameter along the axis, it is found that for each case the diameter decreases monotonically. In order to clarify the power law relation between d and l, the results are replotted in right hand side of Fig. 10 in logarithmic scale. It is clarified that after $l \simeq 100\mu$m, the diameter decreases with almost constant rate. The dash lines are the model estimation obtained by eq. (12) with d_0 set at $l = 100\mu$m. It is found from this figure that the power law of $d_L \sim L^{-1/4}$ slightly overestimates the experimental results. Regression analysis on d_L for $l > 100\mu$m reveals most probable power is about -0.33, which is smaller than the theoretically estimated value of -0.25.

Table 2. Comparison between experimental and theoretical results on ligament break up.

Liquid	L_b	d_L	Oh	d_0 (μm)	
	(μm)	(μm)	number	Measurement	Theory
1	8930	20.8	1.27	60.5	50.8
2	9022	23.8	2.62	62.5	64.4
3	14312	17.1	5.21	64.1	51.4

Breakup into droplets

The stretched ligaments are finally broken up into droplets. For this break up model, we used the ligament breakup model based on Weber's theory. Firstly, the breakup length l_b was determined experimentally from photographs. Then, using the $d_L - l$ relation obtained through regression analysis between $100\mu\text{m} < l < 1000\mu\text{m}$ and the substitution of $l_b$into the$d_L - l$ relation gives the estimation on ligament diameter at breakup length $d_{L,b}$. Finally the diameter of droplets produced are calculated using $d_{L,b}$ with Weber's theory given by Eq. (13).

The droplet diameters are also measured using a particle sizing apparatus based on Fraunhofer diffraction. The measured and estimated droplet diameter are summarized in table 2 along with major parameters used in the model estimation. Here we use D_{10} for characteristic diameter of measured droplets. It is found from this table that the difference in d_0 between theoretical and experimental ones are approximately 10 μm at most which is close to the uncertainty of the present imaging ($\simeq 5\mu$m). It is also noteworthy that the viscous correction through Oh number in Eq. (13) is crucial for the present case where Oh reaches to as high as five; This contributes to produce 35% increase in the model estimation of D.

Summary and Conclusions

Formation and breakup of ligaments from a high-speed rotary bell cup atomizer is observed using short exposure photography with nano pulse flash light. The geometrical properties of ligaments are quantitatively evaluated using image processing. Theoretical models on the formation of root, stretching motion and breakup of ligament are proposed. The major results are summarized as follows: (1)The film spread on the inner surface of the bell cup is split over the groove at the edge of the cup when the thickness of the film is smaller than the depth of the groove. (2) The diameter of ligament root is determined by the width of the split film in the case of lower rotational speed of bell cup, while it is determined by the instability of liquid film on the peripheral edge of cup in the case of higher rotational speed. (3) Simple kinematic model on ligament stretching motion as well as equation of continuity provide good estimation on the thinning rate of ligament diameter along its axis. (4) The breakup model of viscous ligament proposed by Weber gives good estimation on the diameter of droplet of liquids having viscosity from 30 to 100 mPa·s.

References

[1] Tanasawa, Y., Miyasaka, Y., Umehara, M., *Proc 1st International Conference on Liquid Atomization and Spray Systems* 166-172 (1978).
[2] Corbeels, P. L., Senser, D. W., Lefebver, A. H., *Atomization and Sprays* 2: 87-99 (1992).
[3] Kayano, A., Kamiya, T., *Proc 1st International Conference on Liquid Atomization and Spray Systems* 133-138 (1978).
[4] Matsumoto, S., Takashima, Y., *Proc 1st International Conference on Liquid Atomization and Spray Systems* 145-150 (1978).
[5] Ogasawara, S., Daikoku, M., Shirota, M., Inamura, T., Saito, Y., Yasumura, K., Shoji, M., Aoki, H., Miura, T., *Journal of Fluid Science and Technology* 5-3: 464-474 (2010).
[6] Bayvel, L., Orzechowski, Z., *Liquid Atomization* Taylor & Francis, 1993.